J. Appl. Comput. Mech., 7(3) (2021) 1283-1290
DOI: 10.22055/JACM.2020.32261.1992

ISSN: 2383-4536
jacm.scu.ac.ir

Shahid Chamran University of Ahvaz

Journal of Applied and Computational Mechanics

Research Paper

Unsteady Separated Stagnation Point Flow of Nanofluid past a Moving Flat Surface in the Presence of Buongiorno's Model

A. Renuka[1], M. Muthtamilselvan[2], Qassem M. Al-Mdallal[3], D.H. Doh[4], Bahaaeldin Abdalla[5]

[1] Department of Mathematics, Bharathiar University, Coimbatore 641 046, India

[2] Department of Mathematics, Bharathiar University, Coimbatore 641 046, India, Email: muthtamil1@buc.edu.in

[3] Department of Mathematical Sciences, United Arab Emirates University, P. O. Box 15551, Al Ain, Abu Dhabi, United Arab Emirates

[4] Division of Mechanical Engineering, College of Engineering, Korea Maritime and Ocean University, Busan 606 781, South Korea

[5] Department of Mathematics and General Sciences, Prince Sultan University, P.O. Box 66833, Riyadh 11586, Saudi Arabia

Received January 13 2020; Revised May 21 2020; Accepted for publication May 25 2020.
Corresponding author: M. Muthtamilselvan (muthtamil1@buc.edu.in)

Abstract. This paper explores energy and mass transport behavior of unstable separated stagnation point flow of nanofluid over a moving flat surface along with Buongiorno's model. Characteristic of Brownian diffusion and thermophoresis are considered. Additionally, characteristics of chemical reaction is taken into account. A parametric investigation is performed to investigate the outcome of abundant parameters such as temperature, velocity and concentration. An appropriate equation is converting into a set of ODEs through employing appropriate transformation. The governing equations has been solved numerically by using the classical fourth-order Runge-Kutta integration technique combined with the conventional shooting procedure after adapting it into an initial value problem. Our findings depict that the temperature field $\theta(\zeta)$ improves for augmenting values of theromophoresis parameter (Nt) with dual solutions of attached flow without inflection and flow with inflection. Also, the difference of Brownian motion parameter (Nb) with two different solutions of attached flow exists with energy profile. It can be found that an energy profile $\theta(\zeta)$ elevates due to augmenting values of (Nb). It has been perceived that thermal boundary layer thickness elevates due to large amount of Brownian motion parameter (Nb).

Keywords: Stagnation point; Nanofluid; Buongiorno's model.

1. Introduction

Recently, the study of stagnation point flow has an abundant application in many areas including food processing, paper production, polymer extrusion and heat exchanger. Bai et al. [1] presented the MHD Maxwell nanofluid adjoining the stagnation point flow over a stretching surface in the presence of thermophoresis behavior. Wang [2] considered the non-alignment of the stagnation flow towards shrinking sheet. He found that the convective heat transport declines for shrinking rate via elevates in the thickness of boundary layer. Rajappa [3] addressed the unstable plane stagnation point flow along with mass transport. He concluded that the tough blowing at the wall deduced the rate of energy transport and the wall shear stress as well. Saif et al. [4] analyzed the stagnation point flow of second grade nanomaterial towards a nonlinear stretching surface associate with variable surface thickness and energy transport manner is noticed due to the impact of mixed convection and melting heat. They concluded that the concentration and energy fields are hiked with greater thermophoresis parameter.

Nanofluid concept is very first initiated by Choi [5], the mixture of nanometer sized particles suspended in a conventional liquids are ethylene glycol, water or oil. The advantage of this concept is less volume of nanoparticles dispersed in host fluid displays prominent enhancement on the thermal conductivity for energy transport manner. Few wide studies are related to nanofluid flows are available in Refs. [6, 7]. Buongiorno [8] expanded a nanofluid model integrating the influence of thermophoresis and Brownian diffusion. Mustafa et al. [9] addressed the nanofluid flow neighboring a stagnation-point towards a stretching surface by employing the Buongiorno model and analytically solved via homotopy analysis method (HAM). Recently, several researchers have analyzed the Stagnation-point flow in different geometries which can be found in Refs. [10-13]. Kohilavani et al. [14] reported the similarity solutions of the unsteady stagnation-point flow and heat transport of a special third grade fluid over a permeable stretching/shrinking sheet. They found that the stability analysis portrays that the upper branch solution is stable meanwhile the lower branch solution is not stable. Yasin et al. [15] examined the influence of Joule heating, viscous dissipation, partial velocity slip of a viscous and electrically conducting fluid neighborhood of the stagnation point on a stretching/shrinking sheet associated with effect of magnetic field. They found the results for the shrinking sheet there exist

Published online: February 22 2021

non-unique solutions (dual solutions) in particular range of parameters and for the stretching sheet the solution is unique. Numerical studies on different types of biological fluids have been investigated by several researchers [16-18].
An important objective of present work is dealing with an unsteady separated stagnation point flow of nanofluid past a moving flat surface in the presence of energy and mass transport. Furthermore, the effects of chemical reaction are examined. Here, we employed Buongiorno's nanofluid model which includes the thermophoresis and Brownian motion parameter. An appropriate equation is converted from PDEs to ODEs via utilizing proper transformation. Finally, the different parameters' effect on temperature, velocity and concentration are shown in detail.

2. Model Development and Problem Formulation

An unsteady 2-D incompressible flow of nanofluid on the adjoining of stagnation point past a consecutively moving surface along with time dependent external potential flow is considered. The coordinate system and schematic model described in Fig. 1. The schematic system is considered as plate surface in X-axis and Y-axis normal to previous one. The velocity elements (U^*, V^*) are considered in the Cartesian coordinates (X, Y) also time indicated by t. An outer fluid is associated with strain rate volume s(t) > 0 effects on this plate surface in Y-axis. An appropriate equation of a nanofluid along with energy and mass transport under the above assumptions are

$$\frac{\partial U^*}{\partial X}+\frac{\partial V^*}{\partial Y}=0 \tag{1}$$

$$\frac{\partial U^*}{\partial t}+U^*\frac{\partial U^*}{\partial X}+V^*\frac{\partial V^*}{\partial Y}+\frac{1}{\rho}\frac{\partial P^*}{\partial X}=\nu\left(\frac{\partial^2 U^*}{\partial X^2}+\frac{\partial^2 U^*}{\partial Y^2}\right) \tag{2}$$

$$\frac{\partial V^*}{\partial t}+U^*\frac{\partial V^*}{\partial X}+V^*\frac{\partial V^*}{\partial Y}+\frac{1}{\rho}\frac{\partial P^*}{\partial Y}=\nu\left(\frac{\partial^2 V^*}{\partial X^2}+\frac{\partial^2 V^*}{\partial Y^2}\right) \tag{3}$$

$$\frac{\partial T^*}{\partial t}+U^*\frac{\partial T^*}{\partial X}+V^*\frac{\partial T^*}{\partial Y}=\alpha\left(\frac{\partial^2 T^*}{\partial X^2}+\frac{\partial^2 T^*}{\partial Y^2}\right)+\tau\left(D_B\left(\frac{\partial T^*}{\partial X}\frac{\partial C^*}{\partial X}+\frac{\partial T^*}{\partial Y}\frac{\partial C^*}{\partial Y}\right)+\frac{D_T}{T_\infty}\left(\left(\frac{\partial T^*}{\partial X}\right)^2+\left(\frac{\partial T^*}{\partial Y}\right)^2\right)\right) \tag{4}$$

$$\frac{\partial C^*}{\partial t}+U^*\frac{\partial C^*}{\partial X}+V^*\frac{\partial C^*}{\partial Y}=D_B\left(\frac{\partial^2 C^*}{\partial Y^2}\right)+\frac{D_T}{T_\infty}\left(\frac{\partial^2 T^*}{\partial Y^2}\right)-R(C-C_\infty) \tag{5}$$

and also boundary conditions are Dholey [19]:
The boundary conditions due to the consideration that the plate is moving in its own plane with a velocity U_w^* which is λ times of the free stream velocity $U_e^*(X,t)$ are given by

$$\begin{gathered} U_w^*=\lambda U_e^*,\ T^*=T_w^*,\ V^*=0,\ C^*=C_w^* \qquad \text{at} \qquad Y=0, \\ U^*=U_e^*,\ T^*=T_\infty^*,\ C^*=C_\infty^*, \qquad \text{as} \qquad Y\to\infty. \end{gathered} \tag{6}$$

The host equations and conditions are rewritten in the non-dimensional forms, and the used non-dimensional quantities are followed by

$$\begin{gathered} \bar{X}=\frac{X}{L},\ \bar{Y}=\frac{Y}{L},\ \bar{U}^*=\frac{U^*L}{\nu},\ \bar{U}_e^*=\frac{U_e^*L}{\nu},\ \bar{V}^*=\frac{V^*L}{\nu},\ \bar{V}_e^*=\frac{V_e^*L}{\nu}, \\ \bar{t}=\frac{\nu t}{L^2},\ \bar{P}^*=\frac{P^*L^2}{\rho\nu^2},\ \bar{\psi}=\frac{\psi}{\nu},\ \bar{\delta}_1=\frac{\delta_1}{L}. \end{gathered} \tag{7}$$

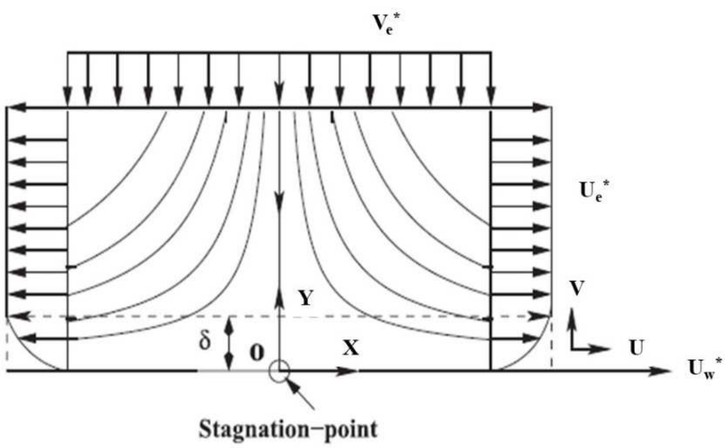

Fig. 1. Schematic configuration of the considered system.

We employed the appropriate similarity variables which can be written as

$$U^{*}=as(t)F'(\zeta),\ V^{*}=a\sqrt{s(t)}F(\zeta),\ \zeta=\sqrt{s(t)}y,\ \theta(\zeta)=\frac{T^{*}-T_{\infty}^{*}}{T_{w}^{*}-T_{\infty}^{*}},\ \phi(\zeta)=\frac{C^{*}-C_{\infty}^{*}}{C_{w}^{*}-C_{\infty}^{*}}. \tag{8}$$

Here, stagnation flow strength indicates $a > 0$. Moreover, an external potential flow point difference manipulated fluid flow inside the boundary layer and also it denotes the time function t. Substitute eq. (7) into the governing equations (1)-(5) along with the boundary conditions (eq. (6)) and using above similarity variables, (eq. (8)), the following equations will be obtained:

$$F''''+aFF'''-aF'F''-\frac{\tilde{s}}{s^{2}}\left(\frac{1}{2}\zeta F'''+\frac{3}{2}F''\right)=0, \tag{9}$$

$$\theta''+\Pr\left(aF\theta'-\beta\frac{\zeta}{2}\theta'+Nt\theta'^{2}+Nb\theta'\phi'\right)=0, \tag{10}$$

$$\phi''+Sc\left(\beta\frac{\zeta}{2}\phi\right)-aF\phi'+\frac{Nt}{Nb}\theta''-ScCr\phi=0. \tag{11}$$

and

$$F(0)=0,\ \theta(0)=1,\ F'(0)=\lambda,\ \phi=1,\ F'(\infty)\to 1,\ F(\infty)\to(\zeta-\delta),\ \theta(\infty)\to 0,\ \phi(\infty)\to 0. \tag{12}$$

From eq. (9), ~ indicates the differentiation with respect to t. Then eq. (9) needs that

$$\frac{\tilde{s}}{s^{2}}=\beta. \tag{13}$$

Let us consider $\beta\neq 0$, necessary condition for comparison of the current study and also integrating above equation as follows

$$s(t)=\frac{1}{\beta(-t+\tau)} \tag{14}$$

Here τ is the steady reference value of time t such that $s(0)=(\tau\beta)^{-1}>0$. If $\beta = 0$, eq. (14) produces s(t) such as unvarying (=1) and also non-dimensional elements of velocity is mentioned in eq. (9) are deduced for stable stagnation-point flow to an inflexible stationary plate highlighted via Hiemenz [13] while $a = 1$. Consequently, the dimensionless parameter β calculates the instability power of this current problem and unstable boundary layer flow detaches from stable flow. Employing eq. (13) into eq. (9)

$$F'''+F''Fa-\beta\left(F'+\frac{1}{2}\zeta F''\right)-aF'^{2}=c, \tag{15}$$

where $c=-(a+\beta)$ by using the boundary condition and applying in above one

$$F'''+aFF''+a-aF'^{2}-\beta\left(\frac{1}{2}\zeta F''-1+F'\right)=0 \tag{16}$$

Consider the analytical solution for $\beta=2a$ through employing a function $G(\zeta)=F(\zeta)-\zeta$ transformation such that

$$F(\zeta)=\zeta+\frac{1-\lambda}{\sqrt{3a+\lambda}}\left(e^{-\sqrt{3a+\lambda}\zeta-1}\right),\quad \text{if}\quad \sqrt{3a=\lambda}>0. \tag{17}$$

For more details refer this article [19] and [20]. The non-dimensional pressure $P(X,\zeta,t)$ distribution is attained by:

$$P(X,\zeta,t)=-\left[\frac{(a+\beta)a}{2\beta^{2}}X^{2}+\frac{a}{\beta(\tau-t)}\left(F'+\frac{a}{2}F^{2}-\frac{\beta}{2}\zeta F\right)\right]+P_{0}(t) \tag{18}$$

where $P_0(t)$ is called stagnation pressure. The stream function ψ is defined as

$$\psi=a\frac{X}{\sqrt{\beta(\tau-t)}}F(\zeta),\qquad \zeta=\frac{Y}{\sqrt{\beta(\tau-t)}}. \tag{19}$$

The engineering interest of in heat and mass transfer flow, local skin friction C_f, local Nusselt number N_u and local Sherwood number S_h are defined by

$$C_{f}=\frac{2}{U_{e}(X,t)^{2}}\left(\frac{\partial U}{\partial Y}\right)_{Y=0}=\frac{2}{a}\frac{1}{X}\sqrt{\beta(\tau-t)}F''(0), \tag{20}$$

$$N_{u}=\frac{X}{T_{w}-T_{\infty}}\left(\frac{\partial U}{\partial Y}\right)_{Y=0}=-\frac{X}{\sqrt{\beta(\tau-t)}}\theta'(0), \tag{21}$$

$$S_{h}=\frac{X}{C_{w}-C_{\infty}}\left(\frac{\partial U}{\partial Y}\right)_{Y=0}=-\frac{X}{\sqrt{\beta(\tau-t)}}\phi'(0), \tag{22}$$

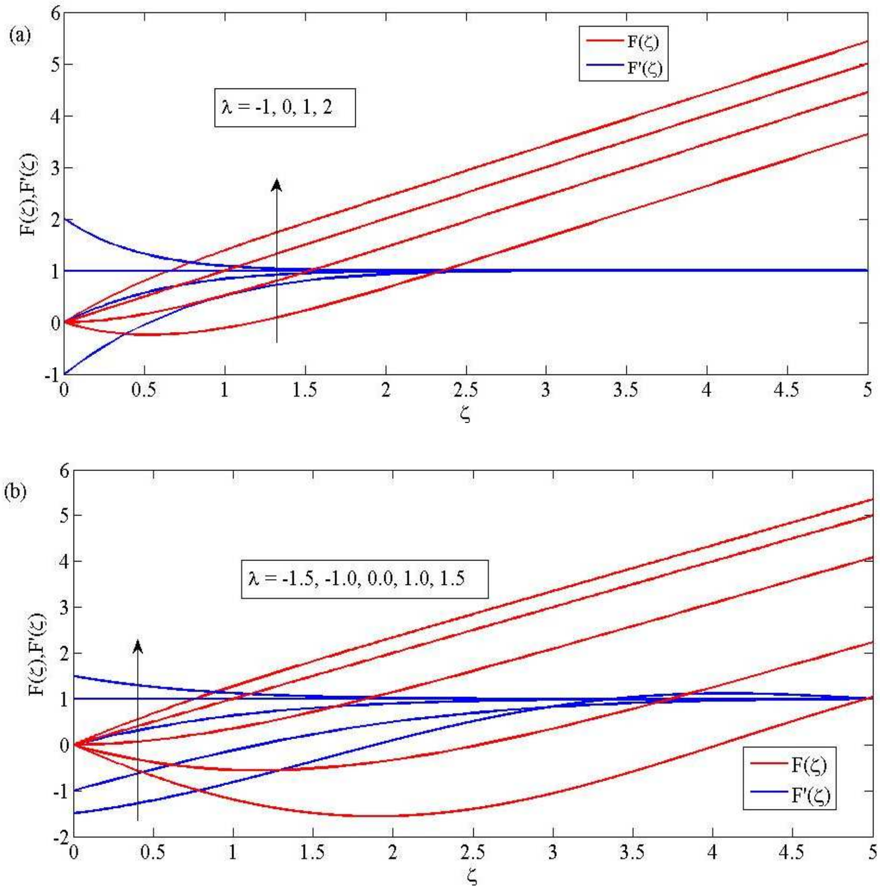

Fig. 2. Difference of F(ζ) and F'(ζ) for various values λ with attached flow solution at (a) β=1 and (b) β=0.

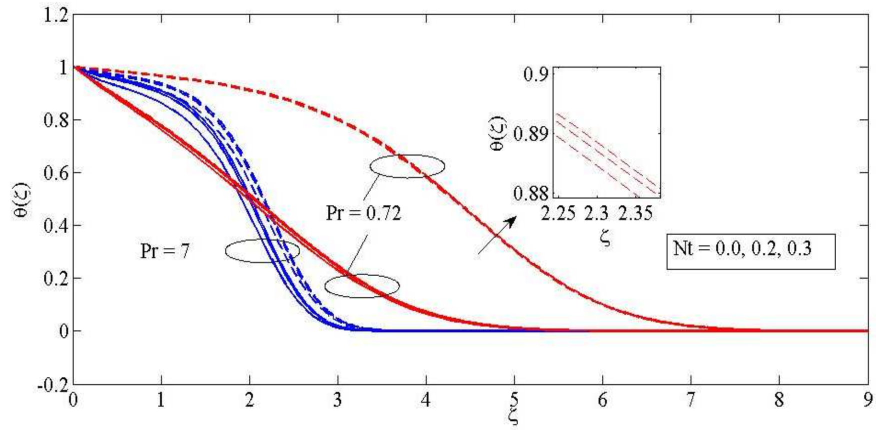

Fig. 3. Difference of θ(ζ) for dual fixed values of Pr=0.72 and 7 when β=0 and λ=-1.2.

3. Result and Discussion

In the current study, the dimensionless ODEs (9)-(11) associate with conditions (eq. (12)) are elucidated numerically via employing RK-method with shooting system. In the current study, our main aim is to notice the impact of different parameters such as velocity ratio parameter λ, unsteadiness parameter β, Brownian motion parameter Nb, chemical reaction parameter Cr, thermophoresis parameter Nt, Schmidt number Sc, Prandtl number Pr on various field of temperature θ(ζ), concentration ϕ(ζ) and velocity F(ζ) respectively.

Figs. 2(a) and 2(b) show the distinct values of unsteadiness in parameter β for an effect of velocity ratio parameter λ on velocity profile F(ζ) and F'(ζ), respectively. There is formation of an inverted boundary layer λ>1 along with λ=0 which denotes the boundary layer having no formation neighboring the surface of plate. The perpendicular element of velocity F(ζ) is computed for velocity ratio parameter λ when β=1 and β=0. It is mainly focused the boundary value flow structure done with the traveling flat surface will have increasing λ. Thus, the velocity F(ζ) elevates in each Fig. 2(a) and Fig. 2(b). Additionally, F'(ζ) represented the horizontal velocity elevates along with augmenting values of λ>0 and F'(ζ) occur to have an inverted the structure of boundary layer meanwhile λ>1 considered for attached flow solution.

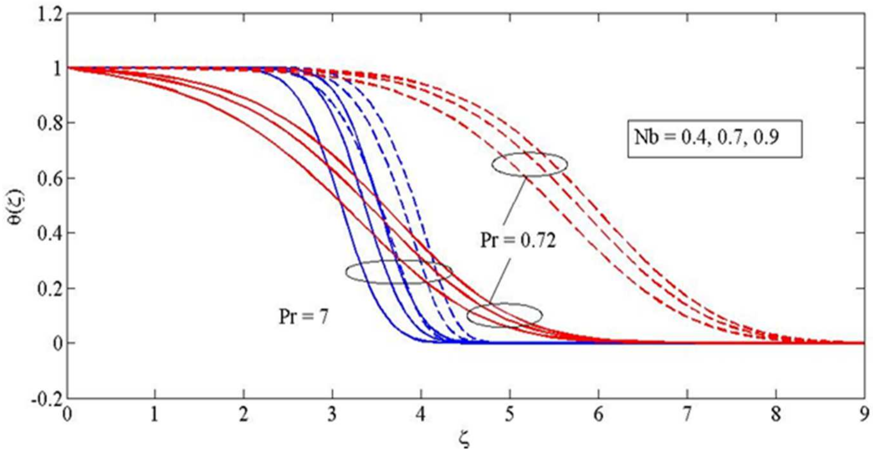

Fig. 4. Difference of θ(ζ) for dual fixed values of Pr=0.72 and 7 when β=0 and λ=-1.2.

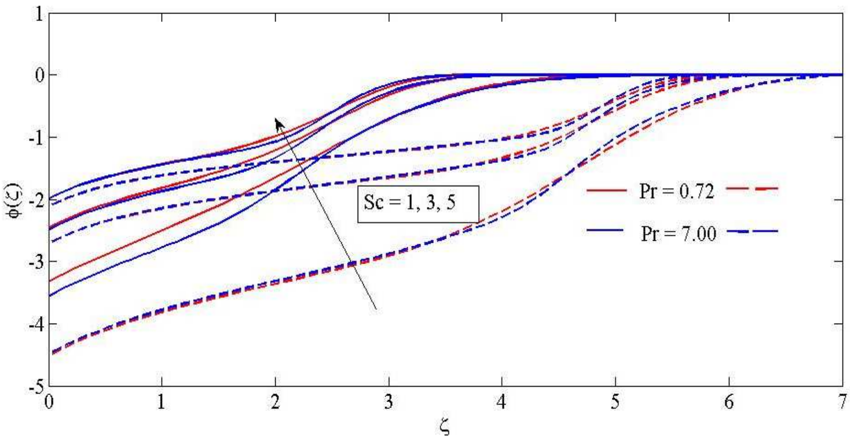

Fig. 5. Difference of ϕ(ζ) for dual fixed values of Pr=0.72 and 7 when β=0 and λ=-1.2.

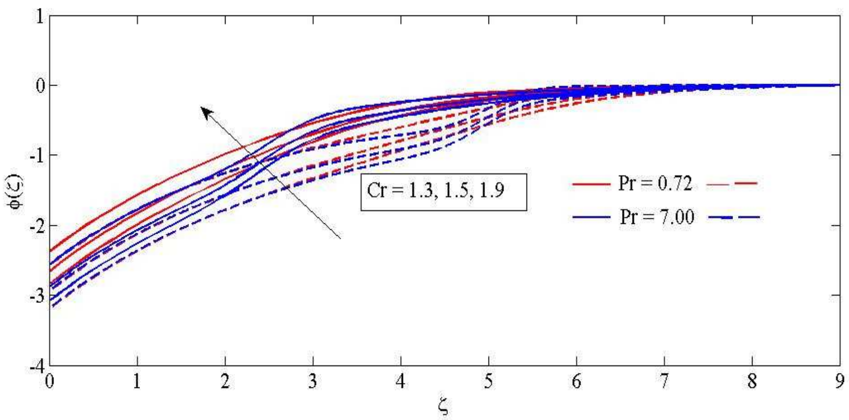

Fig. 6. Difference of ϕ(ζ) for dual fixed values of Pr=0.72 and 7 when β=0 and λ=-1.2.

Figs. 3 and 4 display the temperature distribution of the characteristics of Brownian motion parameter (Nb) and thermophoresis parameter (Nt) for dual constant value of Prandtl number Pr (= 7 for water at 60°F and 0.72 for air) associated to certain amount of β=0 and λ=−1.2 for different attached flow solutions occur. Since, the boundary layer of thermal is higher for flow with an inflection region than the flow without an inflection region. Moreover, the volume of non-dimensional energy slope neighboring the wall, it is larger for flow without an inflection region than the flow with an inflection region. Initially, it can be noticed that thermophoresis parameter have dissimilar values and its leads to different rate of heat transport are explored in Fig. 3. An energy profile θ(ζ) improves with augmenting amount of theromophoresis parameter (Nt) with dual solutions of attached flow without inflection and flow with inflection. It is perceived that the fluid particles and greater thermophoretic force transports from extreme high (warm) to extreme low (cool) temperature core. Secondly, the difference of Brownian motion parameter (Nb) with two different solutions of attached flow exist on temperature profile. It can be found that an energy field θ(ζ) elevates due to augmenting values of Nb. It has been perceived that thermal boundary layer thickness elevates via large amount of Brownian motion parameter (Nb).

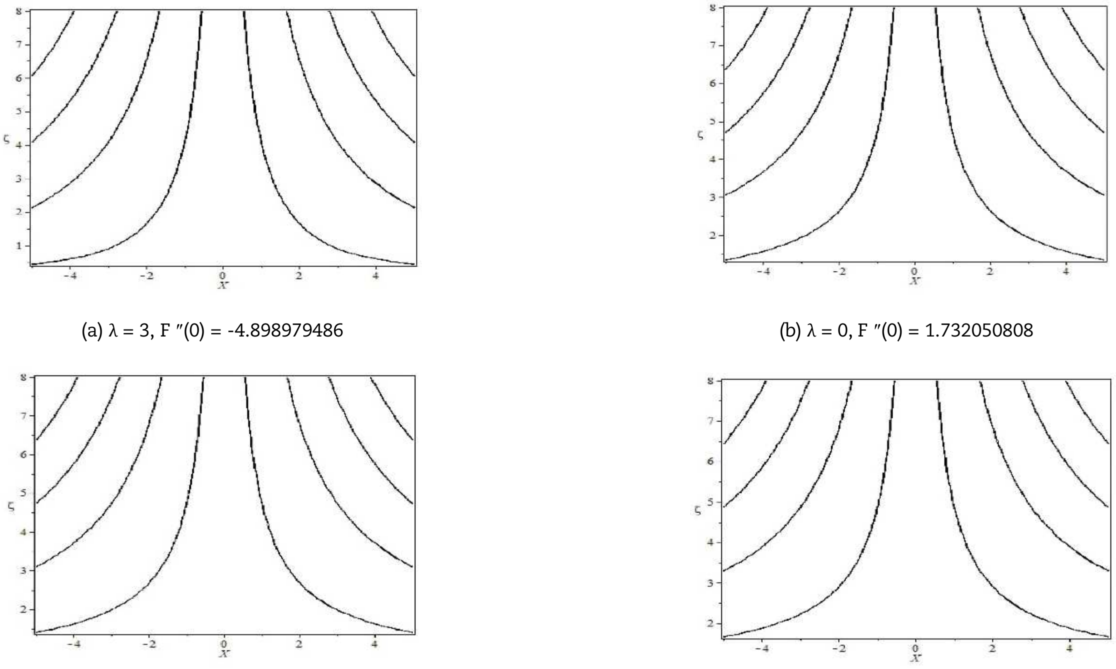

(a) $\lambda = 3$, $F''(0) = -4.898979486$ (b) $\lambda = 0$, $F''(0) = 1.732050808$

(c) $\lambda = -0.1$, $F''(0) = 1.873232501$ (d) $\lambda = -0.5$, $F''(0) = 2.371708245$

Fig. 7. Streamlines depicting attached flow for $\lambda \geq 0$ and reverse flow for $\lambda < 0$ when $\beta = (\tau - 1) = 1$ and a=1. Streamline values change from −2 to 2 in unit increments.

Figs. 5 and 6 demonstrate the concentration distribution of the behavior of chemical reaction parameter (Cr) and Schmidt number (Sc) for dual constant value of Prandtl number Pr (= 7 for water at 60°F and 0.72 for air) associated to certain amount of $\beta=0$ and $\lambda=-1.2$ for different attached flow solutions occur. We noticed that the enhancement of concentration field by increasing value of Schmidt number is presented in Fig. 5. It is led to the concentration decrement and the mass boundary layer thickness increment. Moreover, chemical reaction parameter Cr effect on mass distribution profile is portrayed in Fig. 6. While increasing Cr, the mass profile improves and gives the thinner mass boundary layer thickness.

Figs. 7 and 8 characterize the streamlines flow patterns for different λ over the moving flat surface when a=0.5, 1 and 1.5. The flow pattern reveals the contour of the stream function ψ is mentioned in (19) for different λ when a=0.5 and $(\tau - t) = 1$. It can be found that the streamlines with higher values of λ are minor than the consistent streamlines of $\lambda=0$ and decreasing values of λ. Actually, the streamlines are shifted gradually toward the plate surface with an increasing value of λ, and this trend persists even after the value of $\lambda=1$ for which no boundary layer is formed above the plate surface since $F''(0) = 0$. This indicates the strong attachment of the momentum boundary layer flows to the plate surface which leads to the reduction of the boundary layer thickness as well as to yield the attached flow solution of this flow problem for any given value of $\lambda(>0)$. Moreover, no non-zero saddle point exists within the flow for a positive value of λ. On the other hand, a non-zero saddle point is found inside the flow for a negative value of λ [see Figs. 8(c) and 8(d)]. It is noticeable that this saddle point together with the horizontal dividing streamline ($\psi = 0$) moves away from the plate surface with the increase of $|\lambda|$ when $\lambda < 0$.

In fact, this result has a close relation with the velocity $F(\zeta)$ which decreases continuously with the increase in $|\lambda|$ when $\lambda < 0$ but up to the critical value of λ_c. As a result, the reverse flow zone of $F(\zeta)$ increases so that $F(\zeta)$ becomes zero far away from the plate surface which ensures the detachment of the boundary layer flow to the plate surface. Thus, we see that the detachment of the boundary layer flow enhances with an increasing value of $|\lambda|$ when $\lambda < 0$ and ultimately it must be off the plate surface after a certain negative value of λ depending on the values of β. Finally, we conclude that a positive value of λ, whichever be the value of β, has a strong stabilizing influence on the present unsteady flow dynamics as there exists no non-zero saddle point in this case. This set of graphs indicate the attached flow with greater $\lambda>0$, although it is disconnected from the surface of plate associate to lower $\lambda<0$ comparative to the stable stagnation-point flow $\lambda=0$. Finally, the streamlines are isolated continuously with every values of velocity ratio parameter λ is displayed from Figs. 7 and 8, respectively.

4. Conclusion

The current study deals with the unsteady stagnation point flow of nanofluid past a moving flat surface along with time dependent outer inviscid flow velocity for fixed surface temperature. Characteristics of thermophoresis, Brownian motion and chemical reaction parameter are taken under the consideration. The governing system converted into a system of ODEs employing similarity transformations and the results are carried out through using RK-method along with shooting technique. An important outcome is highlighted:

- $F'(\zeta)$ represented the horizontal velocity elevates along with augmenting values of $\lambda>0$ and $F'(\zeta)$ occur to have an inverted the structure of boundary layer meanwhile velocity ratio parameter $\lambda > 1$ considered for attached flow solution.
- Streamlines pattern represents the flow remains attached with greater $\lambda>0$, and it is disconnected from the surface of plate for lower $\lambda<0$ then comparative to the stable stagnation-point flow $\lambda=0$.
- An energy profile $\theta(\zeta)$ improves while augmenting theromophoresis parameter (Nt) with dual solutions of attached flow without inflection and flow with inflection.
- Concentration distribution are increasing the function of chemical reaction parameter Cr and decreasing functions of Schmidt number Sc.

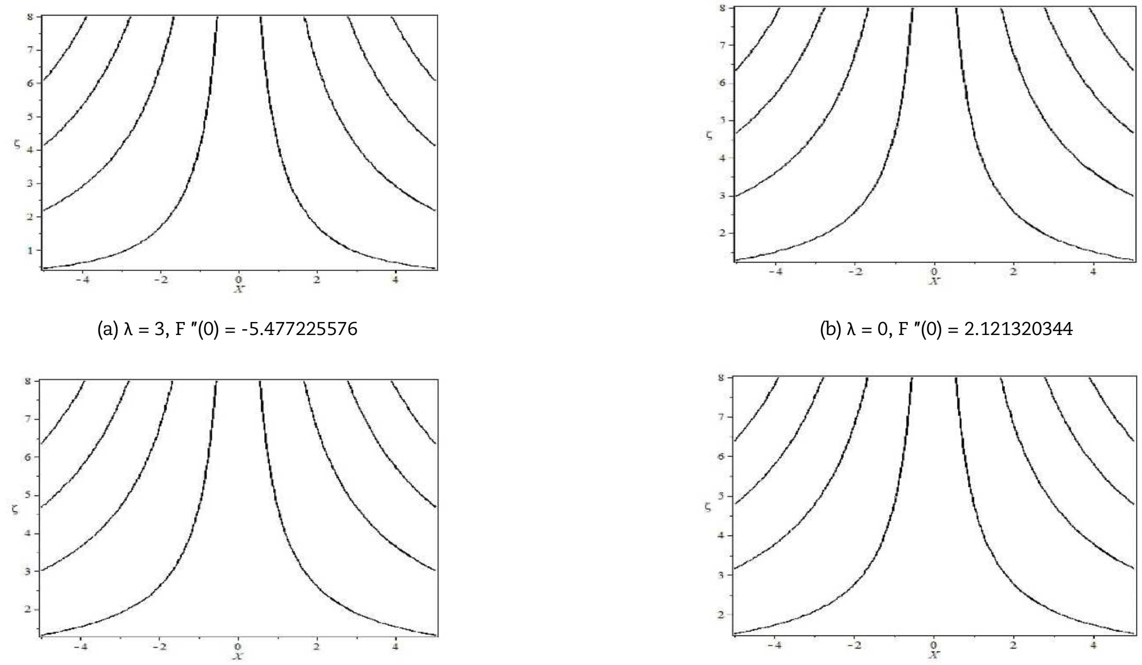

(a) λ = 3, F ″(0) = -5.477225576

(b) λ = 0, F ″(0) = 2.121320344

(c) λ = -0.1, F ″(0) = 2.307379466

(d) λ = -0.5, F ″(0) = 3.0

Fig. 8. Streamlines depicting attached flow for $\lambda \geq 0$ and reverse flow for $\lambda < 0$ when $\beta = (\tau - 1) = 1$ and a=1.5. Streamline values change from –2 to 2 in unit increments.

Author Contributions

The manuscript was written through the contribution of all authors. All authors discussed the results, reviewed and approved the final version of the manuscript.

Acknowledgments

The authors wish to acknowledge the reviewers whose comments helped improve this manuscript.

Conflict of Interest

The authors declared no potential conflicts of interest with respect to the research, authorship and publication of this article.

Funding

The authors would like to acknowledge and express their gratitude to the United Arab Emirates University, Al Ain, UAE for providing the financial support with grant No. 31S363-UPAR(4) 2018. Also, this research was supported by Basic Science Research Program through the National Research Foundation of Korea (NRF) funded by the Korea Government (No. 2017R1A2B2010603). This has been also supported by the Program of Business Cooperative R&D (R0006261) funded by MOTIE. The author would like to thank the Prince Sultan University for funding this work through research group Nonlinear Analysis Methods in Applied Mathematics (NAMAM) group number RG-DES-2017-01-17.

Nomenclature

α	Thermal diffusivity	δ_1	Measure of the displacement thickness
υ	Kinematic viscosity	ψ	Stream function
R	Chemical reaction rate	L	Length scale
D_T	Thermophoresis diffusion coefficient	τ	Propositional of capacity of nanoparticle heat and capacity of fluid heat
T_w^* and T_∞^*	Wall and ambient fluid temperature	C_w^* and C_∞^*	Wall and ambient fluid nanoparticle concentration

References

[1] Bai, Y., Liu, X., Zhang, Y., Zhang, M., Stagnation point heat and mas transfer of MHD Maxwell nanofluids over a stretching surface in the presence of thermophoresis, *Journal of Molecular Liquids*, 224, 2016, 1172-1180.

[2] Wang, C.Y., Stagnation Flow Towards a Shrinking Sheet, *International Journal of Non-Linear Mechanics*, 43(5), 2008, 377-382.

[3] Rajappa, N.R., Non-steady plane stagnation point flow with hard blowing, *Zeitschrift für Angewandte Mathematik und Physik*, 59, 1979, 471-473.

[4] Saif, R.S., Hayat, T., Ellahia, R., Muhammad, T., Alsaedi, A., Stagnation-point flow of second grade nanofluid towards a nonlinear stretching surface with variable thickness, *Results in Physics*, 7, 2017, 2821-2830.

[5] Choi, S.U.S., Enhancing thermal conductivity of fluids with nanoparticles in developments and applications of non-Newtonian flows, *NSiginer HP*

Wang Eds ASME, 66, 1995, 99-105.
[6] Xuan, Y., Li, O., Heat Transfer Enhancement of Nanofluids, *International Journal of Heat Fluid Flow*, 21, 2000, 58-64.
[7] Garoosi, F., Jahanshaloo, L., Rashidi, M.M., Ali, M.E., Numerical simulation of natural convection of the nanofluid in heat exchangers using a Buongiorno model, *Applied Mathematics and Computation*, 254, 2015, 183-203.
[8] Buongiorno, J., Convective transport in nanofluids, *ASME Journal of Heat Transfer*, 128, 2006, 240-250.
[9] Mustafa, M., Hayat, T., Pop, I., Asghare, S., Obaidatc, S., Stagnation-point flow of a nanofluid towards a stretching sheet, *International Journal of Heat and Mass Transfer*, 54, 2011, 5588-5594.
[10] Golafshan, B., Rahimi, A.B., Effects of radiation on mixed convection stagnation-point flow of MHD third-grade nanofluid over a vertical stretching sheet, *Journal of Thermal Analysis and Calorimetry*, 135, 2019, 533–549.
[11] Ijaz Khan, M., Qayyum, S., Waqas, M., Hayat, T., Alsaedi, A., Framing the novel aspects of irreversibility in MHD flow of Williamson nanomaterial with thermal radiation near stagnation point, *Journal of Thermal Analysis and Calorimetry*, 2019, https://doi.org/10.1007/s10973-019-08524-x.
[12] Alizadeh, R., Karimi, N., Nourbakhsh, A., Effects of radiation and magnetic field on mixed convection stagnation-point flow over a cylinder in a porous medium under local thermal non-equilibrium, *Journal of Thermal Analysis and Calorimetry*, 2019, https://doi.org/10.1007/s10973-019-08415-1.
[13] Hiemenz, K., Die grenzschicht an einem in den gleichformigen flussigkeitsstrom eingetauchten geraden kreiszylinder, *Dingl. Polytech. J.*, 326, 1911, 321-410.
[14] Kohilavani, N., Roslinda, N., Pop, I., Unsteady stagnation-point flow and heat transfer of a special third grade fluid past a permeable stretching/shrinking sheet, *Scientific Reports*, 6, 2016, 24632.
[15] Yasin, M.H.M., Ishak, A., Pop, I., MHD stagnation-point flow and heat transfer with effects of viscous dissipation, joule heating and partial velocity slip, *Scientific Reports*, 5, 2015, 17848.
[16]] Nadeem, S., Adel Alblawi, Noor Muhammad, Ibrahim M. Alarifi, AlibekIssakhov, M.T. Mustafa, A computational model for suspensions of motile micro-organisms in the flow of ferrofluid, *Journal of Molecular Liquids*, 293, 2020, 112033.
[17] Nadeem, S., Nadeem Abbas, Yasser Elmasry, M.Y. Malik, Numerical analysis of water based CNTs flow of micropolar fluid through rotating frame, *Computer Methods and Programs in Biomedicine*, 186, 2020, 105194.
[18] Khan, M.N., Nadeem, S., Theoretical treatment of bio-convective Maxwell nanofluid over an exponentially stretching sheet, *Canadian Journal of Physics*, 2019, https://doi.org/10.1139/cjp-2019-0380.
[19] Dholey, S., Unsteady separated stagnation point flow and heat transfer of a viscous fluid over a moving flat surface, *Physics of Fluids*, 30, 2018, 042105.
[20] Dholey, S., Unsteady separated stagnation point flow over a permeable surface, *Zeitschrift für Angewandte Mathematik und Physik*, 70, 2019, 10.

ORCID iD

A. Renuka https://orcid.org/0000-0001-6387-9954
M. Muthtamilselvan https://orcid.org/0000-0003-0075-2520
Qassem M. Al-Mdallal https://orcid.org/0000-0002-2853-9337
D.H. Doh https://orcid.org/00000-0001-6093-2975
Bahaaeldin Abdalla https://orcid.org/0000-0001-8867-0612

How to cite this article: Renuka A., Muthtamilselvan M., Al-Mdallal Q.M., Doh D.H., Abdalla B. Unsteady Separated Stagnation Point Flow of Nanofluid past a Moving Flat Surface in the Presence of Buongiorno's Model, *J. Appl. Comput. Mech.*, 7(3), 2021, 1283–1290. https://doi.org/10.22055/JACM.2020.32261.1992